A reaction class approach for modeling gas phase reaction rates

Thanh N. Truong,* Wendell T. Duncan and Max Tirtowidjojo†

Henry Eyring Center for Theoretical Chemistry, Department of Chemistry, University of Utah, Salt Lake City, Utah 84112, USA

We present a series of new tunneling models based on a reaction class approach. Reaction class consists of all reactions that have the same reactive moiety. One can expect that reactions in the same class share similarities in the shape of the potential energy surfaces along the reaction path. By exploring such similarities, we propose to use reaction path information from the parent (smallest) reaction in calculations of tunneling contributions of larger reactions in the class. This significantly reduces the computational cost while maintaining the accuracy of the model.

I Introduction

One of the great challenges in bridging the gap between chemistry and engineering is providing a complete kinetic model for a given reacting system. Such a kinetic model, in principle, consists of a complete set of various classes of elementary chemical reactions existing in the system along with their thermodynamic and kinetic parameters. The completeness of the kinetic model should not require any assumption regarding the reaction pathways. Despite the growing number of known elementary reaction rate constants, the current kinetic database is far from complete to construct detailed models of most practical industrial reactors. To improve the completeness and accuracy of many kinetic models is a scientific challenge. It is apparent that computational chemistry can play an important role here.

Progress in computational chemistry, particularly development of *ab initio* direct dynamics methods,[1–17] shows promise for predicting accurate thermal rate constants of polyatomic gas-phase reactions. It is now possible to calculate rate constants for reactions of moderate size (less than 20 atoms). However, many practical kinetic models consist of thousands of elementary reactions. To date, the main source of getting these rate constants theoretically is from the framework of conventional transition state theory (TST). The TST methodology has known deficiencies. In particular, it does not include the recrossing effects that are important in the high temperature region and cannot adequately model the quantum mechanical tunneling effects that are significant in the low temperature region in many combustion reactions. Unfortunately, to obtain a more accurate tunneling contribution, more potential energy information is needed. A better theoretical approach is the variational transition state theory (VTST)[18–24] augmented by semiclassical multidimensional small-curvature tunneling corrections,[22,25] This requires energy, gradient, and Hessian information along the reaction path. This information can be costly to calculate, particularly for large systems. In this study, we introduce an approach that allows more accurate rate constants to be estimated at little additional cost beyond that of TST calculations.

The central idea of this approach is based on the following realization. Reactions in a kinetic model are categorized in classes (sometimes referred to as reaction types). Reactions in the same class have the same reactive moiety, thus are expected to have similarities in their potential energy surfaces along their reaction valleys. For the parent reaction, defined to be the smallest reaction in the class, we can calculate its potential surface information accurately without much computational cost. In many cases, such information is already available from previous studies. It is possible to transfer such information in rate calculations of larger reactions without having to compute it explicitly. Consequently, this will reduce the computational cost significantly. It is important to point out that the reaction class idea is quite general, however, in this study we will focus on its use in calculating quantum mechanical tunneling effects. We will explore its uses for other components of rate constants in future studies.

II Methodology

Within the framework of TST and VTST, motion along the reaction coordinate is treated classically while vibrational motions perpendicular to this degree of freedom are treated quantum mechanically. Quantum mechanical effects in the reaction coordinate motion are represented by the temperature dependent transmission coefficient $\kappa(T)$. This coefficient accounts for both the non-classical reflection when the total energy of the system is above the barrier and the tunneling effects when the energy is below the threshold barrier. However, as shown below tunneling is the dominant factor of the two.

Within the TST formalism, the tunneling effect can be estimated from the Wigner correction which depends only on the imaginary frequency of the transition state. It is known that the Wigner correction often grossly underestimates the tunneling effect since it only accounts for contributions near the top of the barrier. More accurate treatments of tunneling effects require potential information along the tunneling path. Within the centrifugal-dominant small-curvature semiclassical adiabatic ground-state approximation,[25] the effective potential for tunneling can be approximated by the vibrationally-adiabatic ground-state potential given by

$$V_a^G(s) = V_{MEP}(s) + V_{int}(s) \tag{1}$$

where $V_{MEP}(s)$ is the potential energy along the minimum energy path; $V_{int}(s)$ denotes the total zero-point energy at s

$$V_{int}(s) = \sum_{i=1}^{3N-7} \frac{1}{2} \hbar\omega_i(s) \tag{2}$$

with ω_i denoting the frequency of mode i and the sum is overall vibrational modes orthogonal to the reaction coordinate at s. Here the reaction coordinate s is defined as the distance along the minimum energy path with the origin located at the transition state and the positive direction toward the product. From the multidimensional semiclassical centrifugal-dominant small curvature tunneling (SCT) method the transmission coefficient is approximated as the ratio of the thermally averaged multidimensional semiclassical transmission probability $P(E)$ to the thermally averaged classical transmission probability for scattering by the effective potential $V_a^G(s)$ and it is given by

$$\kappa(T) = \frac{\int_0^\infty P(E)\mathrm{e}^{\{-E/k_bT\}}\,\mathrm{d}E}{\int_{E^*(T)}^\infty \mathrm{e}^{\{-E/k_bT\}}\,\mathrm{d}E} \tag{3}$$

where k_b is the Boltzmann constant, $E^*(T)$ denotes the value of V_a^G at the bottleneck. The transmission probability $P(E)$ is expressed as

$$P(E) = \frac{1}{(1 + \mathrm{e}^{2\theta(E)})} \tag{4}$$

where $\theta(E)$ is the imaginary action integral evaluated along the tunneling path and is expressed as

$$\theta(E) = \frac{2\pi}{h} \int_{s_1}^{s_r} \sqrt{2\mu_{\mathrm{eff}}(s)\,|E - V_a^G(s)|}\,\mathrm{d}s \tag{5}$$

where s_1 and s_r are the reactive classical turning points, and $\mu_{\mathrm{eff}}(s)$ is the effective reduced mass that includes the reaction path curvature, *i.e.* corner cutting effects. The explicit expression for it is not critical for this discussion and can be found elsewhere.[25] In order to calculate the transmission coefficient one needs to determine $V_a^G(s)$ and $\mu_{\mathrm{eff}}(s)$. These two terms require energy, gradient and Hessian information along the reaction coordinate. Calculating this information particularly for the Hessians is quite computationally demanding. Below we describe several reaction class models for approximating the $V_a^G(s)$ and $\mu_{\mathrm{eff}}(s)$ terms. For the purpose of comparison we also briefly describe the Eckart model that we proposed earlier.[26]

A Eckart model

The Eckart model is based on two fundamental approximations. *Approximation 1*: Neglecting the corner cutting effects, *i.e.* $\mu_{\mathrm{eff}}(s) = \mu$. The reduced mass μ is equal to 1 u if the minimum energy path is calculated in the mass-weighted Cartesian coordinate. Thus, the accuracy of the model should be compared to the zero-curvature tunneling (ZCT)[22] case. *Approximation 2*: $V_a^G(s)$ is described by an Eckart function going through three points, namely the reactant(s), transition state, and product(s). The width of this function is assumed to be the same as of the V_{MEP} that is obtained from fitting the V_{MEP} to another Eckart function using potential energy information at the reactant(s), transition state, and product(s) and the imaginary frequency of the transition state.

Since the zero-point energy correction often lowers the classical barrier height, consequently it leads to larger potential width for $V_a^G(s)$ as compared to that of the classical potential curve. Thus, assuming both potential curves have the same width the tunneling contribution will be overestimated. The error, however, sometimes can compensate for the corner cutting effects that are not included in the Eckart formalism. As a result, good agreement with experimental data was sometimes obtained.[26,27]

B Reaction class models

The reaction class approach is based on one fundamental postulate: all reactions in the same class share certain similarities on their potential surfaces along their reaction coordinates. The models given below not only describe a hierarchy of approximations but are also designed to test the above postulate. These models assume that $V_a^G(s)$ and $\mu_{\mathrm{eff}}(s)$ functions for the parent reaction, *i.e.* the smallest reaction in the class, are available. Due to the size of the parent reaction, these functions can be easily obtained. In all reaction class tunneling models, we assume that $\mu_{\mathrm{eff}}(s)$ is the same for all reactions in the class, *i.e.* the reaction path curvature is the same. Since the reaction path curvature components are largest for the reactive modes which result mainly from motions of atoms in the reactive moiety, this approximation is quite reasonable. Furthermore, from detailed analysis we found that the transmission coefficient is much more sensitive to the $V_a^G(s)$ potential than the effective reduced mass $\mu_{\mathrm{eff}}(s)$.

B.1 Model RC-μV. This model is based on two fundamental approximations. *Approximation 1*: $\mu_{\mathrm{eff}}(s)$ is the same for all reactions in the class. *Approximation 2*: $V_a^G(s)$ has similar shape for all reactions in the class. Thus, $V_a^G(s)$ for a specific reaction can be obtained by scaling the $V_a^G(s)$ of the parent reaction to have the correct barrier.

This model requires only energy and frequency information at the reactant(s), transition state, and product(s) for the specific reaction.

B.2 Model RC-μi. Initial study indicates that the transmission coefficient is very sensitive to the $V_a^G(s)$ potential but not the $\mu_{\mathrm{eff}}(s)$. This model is designed to improve the approximation used in the model RC-μV and also has two approximations. *Approximation 1*: $\mu_{\mathrm{eff}}(s)$ is the same for all reactions in the class. *Approximation 2*: Reactions in the same class have a similar width in the directions perpendicular to the reaction coordinate. This means $V_{\mathrm{int}}(s)$ for a specific reaction can be obtained from scaling that of the parent reaction to go through the value at the transition state. Conseqently, $V_a^G(s)$ is determined from the calculated V_{MEP} and the scaled $V_{\mathrm{int}}(s)$.

This model requires not only energy and frequency information at the reactant(s), transition state and product(s) but also the potential energy V_{MEP} along the minimum energy path.

III Test cases

We have selected a class of hydrogen abstraction reactions to test the proposed reaction class approach. These reactions are

$$\mathrm{H + H{-}CH_3 \rightarrow H_2 + CH_3} \tag{R1}$$

$$\mathrm{H + H{-}CH_2F \rightarrow H_2 + CH_2F} \tag{R2}$$

$$\mathrm{H + H{-}CHF_2 \rightarrow H_2 + CHF_2} \tag{R3}$$

$$\mathrm{H + H{-}CF_3 \rightarrow H_2 + CF_3} \tag{R4}$$
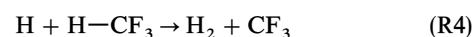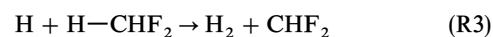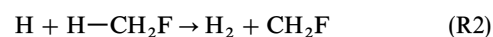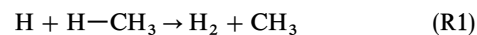
The reactive moiety for this class of reaction is $\mathrm{H + H{-}C}$. Using the large electronegative F as substituents is expected to have substantial effects on the reaction path information of these reactions. Reactions R1 and R4 both have co-linear-like C_{3v} reaction paths, *i.e.* the H–H–C angle is 180°, whereas the reaction paths of R2 and R3 reactions no longer have such symmetry. In fact, at the transition state, the H–H–C angle is distorted from the linear configuration by 0.7° for R2 and 1.8° for R3 (see Table 1). The distortions in the reaction paths of R2 and R3 relative to that of the parent reaction R1 provide severe tests on the proposed methodology. Note that the reac-

Table 1 Geometrical parameters of the transition states (bond lengths in Å, angle in degrees) and classical barrier heights (kcal mol^{-1}) for the selected hydrogen abstraction reactions
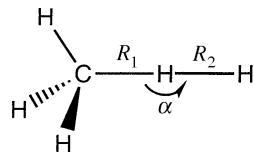
	R1	R2	α	$\Delta V^{\ddagger}$
$H + CH_4$	1.4154	0.8965	180	12.44
$H + CH_3F$	1.3686	0.9308	177	10.29
$H + CH_2F_2$	1.3648	0.9325	176	10.27
$H + CHF_3$	1.4118	0.8971	180	13.46

tions R1–R4 have noticeable electronic substituent effects as the barriers vary from 10.3 to 13.5 kcal mol^{-1} as listed in Table 1. In this study, we are only interested in testing the accuracy of the reaction class tunneling models therefore we will focus on the accuracy of the transmission coefficients rather than on the absolute rate constants. Accurate rate calculations for these reactions are presented in a separate paper.[28]

IV Computational details

All electronic structure calculations were done using hybrid non-local BH&H[29]–LYP[30] density functional theory with the cc-pVDZ basis set. Since we are not interested in the accuracy of the absolute rate, this level of theory is sufficient for our purpose. Minimum energy paths (MEP) were calculated in mass-weighted Cartesian coordinates with the step size of 0.01 u$^{1/2}$ a_0 using the Gonzalez–Schlegel method.[31] A total of 23 Hessian points were calculated with the grid locations selected according to our focusing technique.[32] All electronic structure calculations were done using the G94 program.[33] Rate calculations were carried out using our TheRate program.[32]

V Results and discussion

First we examine the generalized frequencies along the reaction coordinates shown in Fig. 1. Note that these four reactions do exhibit similarity in the locations where the active frequency modes experience large changes. These locations also correspond to positions along the reaction coordinates where the potential surfaces have large curvatures. As a consequence, more corner cutting effects occur in these regions which correspond to smaller μ_{eff}. This point is further supported by the plots of the effective reduced mass as a function of the reaction coordinate as shown in Fig. 2. In Fig. 2b and c, results for the parent reaction $H + CH_4$ are also plotted in dashed lines for comparison. Despite the distortion in the reaction paths of R2 and R3, all four reactions have remarkably similar effective reduced mass as a function of the reaction coordinate. These results support our first assumption in both reaction class models.

The zero-point energy corrected potential curves, V_a^{G}, for R1–R4 are plotted in Fig. 3. The Eckart potential curves for the Eckart model and the approximated V_a^{G} potential curves for the RC-μV and RC-μi models are also plotted in Fig. 3b–d. First, the Eckart curves have much narrower width compared to the "exact" results. Consequently, it leads to an important implication for calculations of the transmission coefficient as discussed below. The approximated V_a^{G} curves agree much better with the results from full calculations, though there are some differences in the two models. These differences are due to the electronic effects of strong electro-
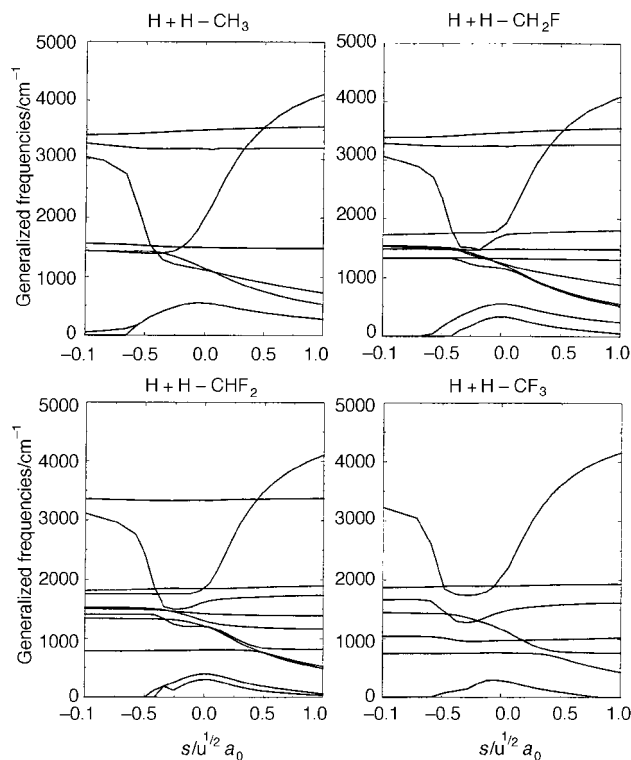
Fig. 1 Plots of generalized frequencies (cm^{-1}) as functions of the reaction coordinate for R1–R4 reactions as indicated.

negative substituents on the reactive moiety. As seen from eqn. (5), this will certainly lead to noticeable error in the calculated transmission coefficients. The approximated V_a^{G} curves for the RC-μi model calculated by adding the scaled V_{int} potential to the exact V_{MEP} potential show the best agreement with the exact results. In this case, the electronic effects from the spectator region is explicitly accounted for in the V_{MEP}.

Calculated transmission coefficients for R2–R4 are listed in Tables 2–4. SCT results provide the most accurate estimations for tunneling contributions considered here. First of all, Wigner corrections, κ_{W}, significantly underestimate tunneling
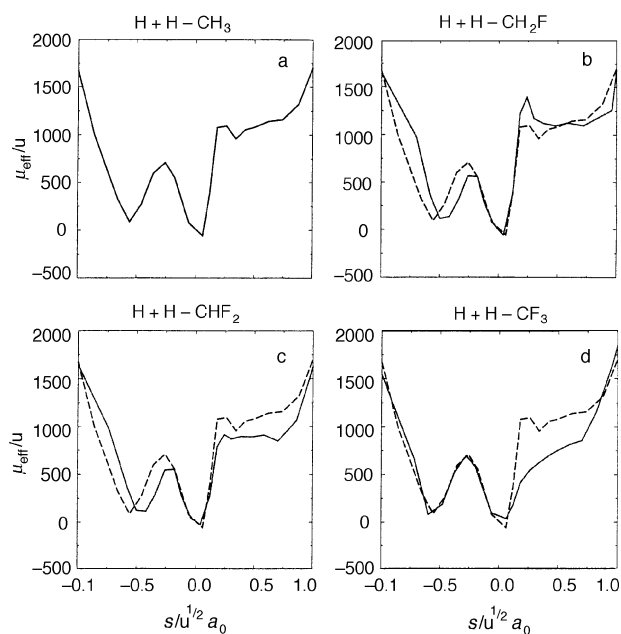
Fig. 2 Plots of the effective reduced mass μ_{eff} (u) as functions of the reaction coordinate for R1–R4 reactions as indicated. μ_{eff} of the parent $H + CH_4$ reaction (dashed lines) is superimposed with those of the R2–R4 reactions for comparsion.
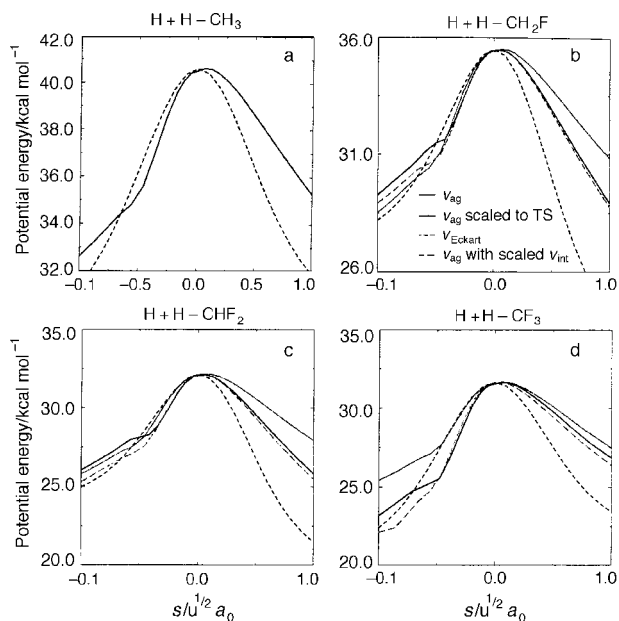
Fig. 3 Plots of the V_a^G potential curves as functions of the reaction coordinate for R1–R4 reactions as indicated. Solid lines are the results from full calculations. Short-dashed lines are from the Eckart model, dotted lines are from the RC-μV model and long-dashed lines are from the RC-μi model.

in all cases particularly below room temperature. Since recent studies have shown the Eckart model to be quite accurate in predicting tunneling contributions, it is worth re-examining the accuracy of this model. Since the Eckart tunneling model does not include the corner cutting effects, it should be compared with the corresponding "exact" zero-curvature tunneling (ZCT) results. Note that due to the narrow widths of the Eckart potentials, this model overestimates the tunneling contributions in all cases by more than a factor of 2 at room

temperature. However, when comparing with the SCT results, we can confirm our earlier conclusion that these errors compensate for the corner cutting effects not included in the model.[26,27] Our present results caution the interpretation of the success of the Eckart model. Recall that in the reaction class tunneling models, the corner cutting effects are explicitly included. Different RC models provide different levels of complexity in approximating the effective potential for tunneling. In the RC-μV model, the V_a^G potential for tunneling is obtained from scaling that of the parent reaction. From Fig. 3b–d, the scaled V_a^G curves are more accurate than the Eckart curves; however, the potential widths are overestimated. As a result, the RC-μV model underestimates the tunneling contribution noticeably. For the RC-μi model, in addition to the information at the stationary points, the V_{MEP} potential is also required. We obtained the V_a^G potential by adding the scaled V_{int} to the "exact" V_{MEP} potential. This provides a significant improvement over the RC-μV model and yields the best agreement with the "exact" SCT results. The error is less than 34% at room temperature for all cases. This is remarkable considering that the computational cost involved is much less than full SCT calculations.

VI Conclusion

We present new tunneling models that are based on a reaction class idea. This idea recognizes that reactions in the same class have the same reactive moiety and thus share similar features on their potential energy surfaces along their minimum energy paths. By exploring these similarities and the sensitivity of the tunneling calculations, we proposed two RC tunneling models that allow usage of potential information from the parent reaction (the smallest reaction in the class) that is often available or can be obtained cheaply. Compared to the full "exact" results, these new models give more than an order of magnitude improvement in the performance. An encouraging fact is that the reaction class idea is quite general and is not limited to the above usage in calculating tunneling contributions. We will explore such possibilities for calculating other components of rate constants in future studies.

References

1 K. K. Baldridge, M. S. Gordon, D. G. Truhlar and R. Steckler, *J. Phys. Chem.*, 1989, **93**, 5107.
2 B. C. Garrett, M. L. Koszykowski, C. F. Melius and M. Page, *J. Phys. Chem.*, 1990, **94**, 7096.
3 B. C. Garrett and C. F. Melius, in *Theoretical and Computational Models for Organic Chemistry*, ed. S. J. Formosinho, I. G. Csizmadia and L. G. Arnaut, Kluwer, Dordrecht, 1991, pp. 25–54.
4 A. Gonzalez-Lafont, T. N. Truong and D. G. Truhlar, *J. Chem. Phys.*, 1991, **95**, 8875.
5 W-P. Hu, Y-P. Liu and D. G. Truhlar, *J. Chem. Soc., Faraday Trans.*, 1994, **90**, 1715.
6 Y-P. Liu, G. C. Lynch, T. N. Truong, D-h. Lu and D. G. Truhlar, *J. Am. Chem. Soc.*, 1993, **115**, 2408.
7 Y-P. Liu, D-h. Lu, A. Gonzalez-Lafont, D. G. Truhlar and B. C. Garrett, *J. Am. Chem. Soc.*, 1993, **115**, 7806.
8 K. A. Nguyen, I. Rossi and D. G. Truhlar, *J. Chem. Phys.*, 1995, **103**, 5522.
9 D. G. Truhlar, in *The Reaction Path in Chemistry: Current Approaches and Perspectives*, ed. D. Heidrich, Kluwer Academic, 1995, p. 229.

Table 2 Calculated transmission coefficients for $H + CH_3F$ reaction

T/K	κ_{SCT}	κ_{ZCT}	κ_w	κ_{Eckart}	$\kappa_{RC-\mu V}$	$\kappa_{RC-\mu i}$
250	151.69	12.64	4.41	49.50	32.47	200.45
300	32.85	5.14	3.36	12.04	10.77	39.43
400	6.72	2.17	2.33	3.36	3.47	7.36
500	3.16	1.45	2.05	1.93	2.02	3.33
600	2.06	1.15	1.59	1.42	1.48	2.14
800	1.31	0.90	1.33	1.03	1.06	1.34

Table 3 Calculated transmission coefficients for $H + CH_2F_2$ reaction

T/K	κ_{SCT}	κ_{ZCT}	κ_w	κ_{Eckart}	$\kappa_{RC-\mu V}$	$\kappa_{RC-\mu i}$
250	246.26	13.12	4.54	45.12	20.91	228.60
300	51.37	5.39	3.46	11.47	7.97	43.69
400	9.55	2.26	2.38	3.30	2.94	7.88
500	4.14	1.50	1.88	1.91	1.81	3.50
600	2.56	1.18	1.61	1.41	1.37	2.23
800	1.52	0.91	1.35	1.02	1.01	1.38

Table 4 Calculated transmission coefficients for $H + CHF_3$ reaction

T/K	κ_{SCT}	κ_{ZCT}	κ_w	κ_{Eckart}	$\kappa_{RC-\mu V}$	$\kappa_{RC-\mu i}$
250	151.59	8.24	4.01	35.68	19.88	83.155
300	32.85	3.76	3.09	9.27	7.68	21.66
400	6.72	1.79	2.18	2.88	2.88	5.35
500	3.16	1.26	1.75	1.74	1.79	2.72
600	2.06	1.04	1.52	1.32	1.35	1.85
800	1.31	0.83	1.29	0.98	1.00	1.23

10 T. N. Truong, *J. Chem. Phys.*, 1994, **100**, 8014.
11 T. N. Truong and W. T. Duncan, *J. Chem. Phys.*, 1994, **101**, 7408.
12 T. N. Truong and T. J. Evans, *J. Phys. Chem.*, 1994, **98**, 9558.
13 T. N. Truong, *J. Chem. Phys.*, 1995, **102**, 5335.
14 R. Bell and T. N. Truong, *J. Chem. Phys*, 1994, **101**, 10442.
15 W. T. Duncan and T. N. Truong, *J. Chem. Phys.*, 1995, **103**, 9642.
16 T. N. Truong, W. T. Duncan and R. L. Bell, in *Chemical Applications of Density Functional Theory*, ed. B. B. Laird, R. B. Ross and T. Ziegler, American Chemical Society, Washington DC, 1996, vol. 629, p. 85.
17 J. C. Corchado, E. L. Coitino, Y-Y. Chuang, P. L. Fast and D. G. Truhlar, *J. Phys. Chem. A*, 1998, **102**, 2424.
18 B. C. Garrett and D. G. Truhlar, *J. Chem. Phys.*, 1979, **70**, 1593.
19 D. G. Truhlar and B. C. Garrett, *Acc. Chem. Res.*, 1980, **13**, 440.
20 D. G. Truhlar, A. D. Isaacson, R. T. Skodje and B. C. Garrett, *J. Phys. Chem.*, 1982, **86**, 2252.
21 D. G. Truhlar and B. C. Garrett, *Annu. Rev. Phys. Chem.*, 1984, **35**, 159.
22 D. G. Truhlar, A. D. Isaacson and B. C. Garrett, in *Theory of Chemical Reaction Dynamics*, ed. M. Baer, CRC Press, Boca Raton, FL, 1985, vol. 4, pp. 65–137.
23 D. G. Truhlar and B. C. Garrett, *J. Chim. Phys.*, 1987, **84**, 365.
24 S. C. Tucker and D. G. Truhlar, in *New Theoretical Concepts for Understanding Organic Reactions*, ed. J. Bertran and I. G. Csizmadia, Kluwer, Dordrecht, Netherlands, 1989, pp. 291–346.
25 D-h. Lu, T. N. Truong, V. S. Melissas, G. C. Lynch, Y. P. Liu, B. C. Garrett, R. Steckler, A. D. Isaacson, S. N. Rai, G. C. Hancock, J. G. Lauderdale, T. Joseph and D. G. Truhlar, *Comput. Phys. Commun.*, 1992, **71**, 235.
26 T. N. Truong and D. G. Truhlar, *J. Chem. Phys.*, 1990, **93**, 1761.
27 T. N. Truong, *J. Phys. Chem. B*, 1997, **101**, 2750.
28 D. K. Maity, W. T. Duncan and T. N. Truong, *J. Phys. Chem. A*, 1999, in press.
29 A. D. Becke, *J. Chem. Phys.*, 1993, **98**, 1372.
30 C. Lee, W. Yang and R. G. Parr, *Phys. Rev. B*, 1988, **37**, 785.
31 C. Gonzalez and H. B. Schlegel, *J. Phys. Chem.*, 1990, **94**, 5523.
32 W. T. Duncan, R. L. Bell and T. N. Truong, *J. Comput. Chem.*, 1998, **19**, 1039 (also: http://therate.hec/utah.edu).
33 M. J. Frisch, G. W. Trucks, H. B. Schlegel, P. M. W. Gill, B. G. Johnson, M. A. Robb, J. R. Cheeseman, T. A. Keith, G. A. Petersson, J. A. Montgomery, B. Raghavachari, M. A. Al-Laham, V. G. Zakrzewski, J. V. Ortiz, J. B. Foresman, J. Cioslowski, B. Stefanov, A. Nanayakkara, M. Challacombe, C. Y. Peng, P. Y. Ayala, W. Chan, M. W. Wong, J. L. Andres, E. S. Replogle, R. Gomperts, R. L. Martin, D. J. Fox, J. S. Binkley, D. J. Defrees, J. Baker, J. P. Stewart, M. Head-Gordon, C. Gonzalez and J. A. Pople, GAUSSIAN94, B.1 edn., Gaussian, Inc., Pittsburgh, 1995.

Paper 8/08438F